Electronic Supporting Information

Polyyne Bridged AIE Luminogen with Red Emission: Design, Synthesis, Property and Application

Zheng Zhao,[†bc] Huifang Su,[†a] Pengfei Zhang,[bc] Yuanjing Cai,[bc] Ryan T. K. Kwok,[bc] Yuncong Chen,[bc] Zikai He,[bc] Xinggui Gu,[bc] Xuewen He,[bc] Herman H. Y. Sung,[b] Ian D. Williams,[b] Jacky W. Y. Lam,[bc] Zhenfeng Zhang*,[a] and Ben Zhong Tang*,[bcd]

[a]Sun Yat-Sen University Cancer Center, State Key Laboratory of Oncology in South China, Collaborative Innovation Center for Cancer Medicine, Guangzhou 510060, China.

[b]Department of Chemistry, Hong Kong Branch of Chinese National Engineering Research Center for Tissue Restoration and Reconstruction, Institute of Molecular Functional Materials, Institute for Advanced Study, State Key Laboratory of neuroscience, Division of Biomedical Engineering, and Division of Life Science, The Hong Kong University of Science and Technology, Clear Water Bay, Kowloon, Hong Kong, China.

[c]HKUST-Shenzhen Research Institute, No. 9 Yuexing 1st RD, South Area, Hi-tech Park, Nanshan, Shenzhen 518057, China

[d]Guangdong Innovative Research Team, SCUT-HKUST Joint Research Laboratory, State Key Laboratory of Luminescent Materials and Devices, South China University of Technology, Guangzhou 510640, China

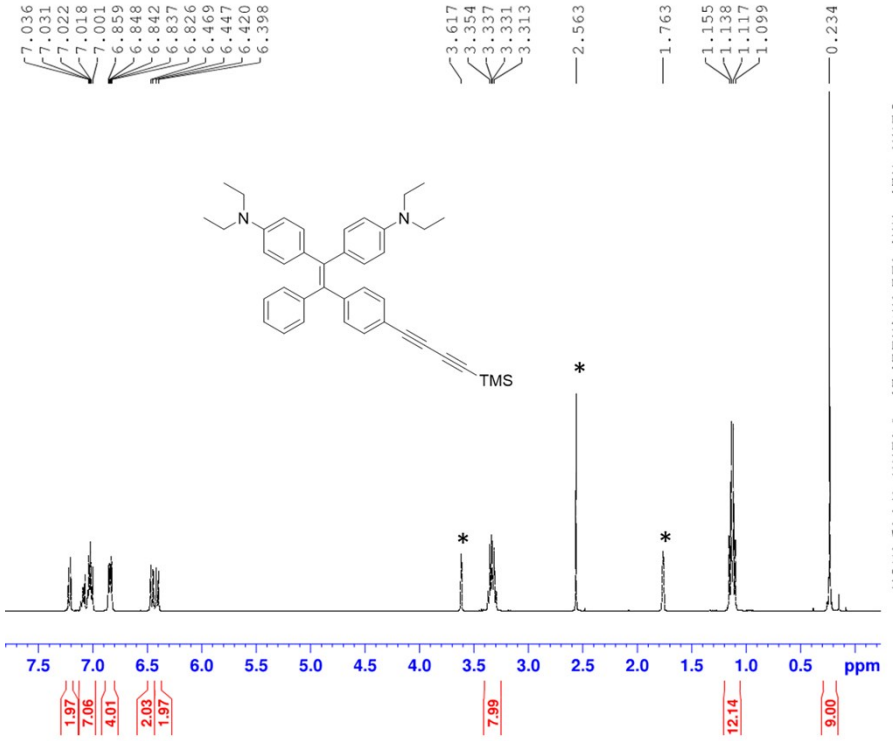

Figure S1. ^{1}H NMR spectrum of compound **2** inTHF-d_8.

Note: for all the following ^{1}H NMR and ^{13}CNMR spectra, the symbol of * represents the signals of THF-d_8

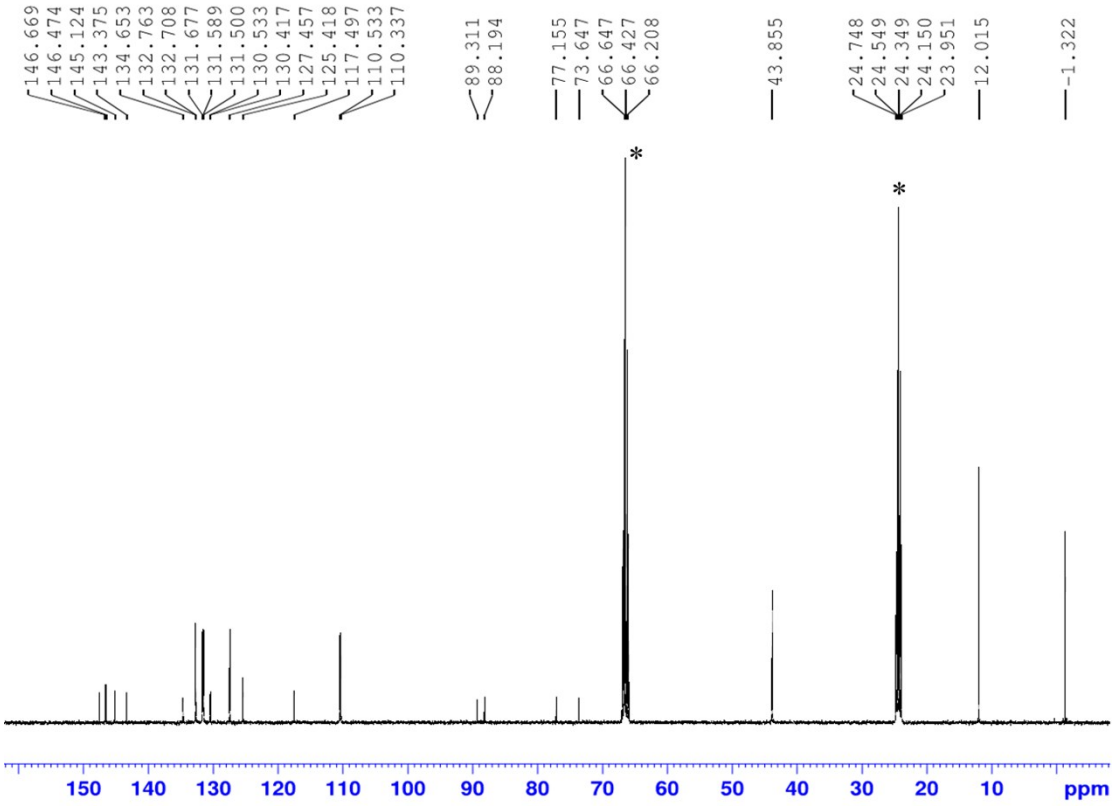

Figure S2. ^{13}C NMR spectrum of compound **2** inTHF-d_8.

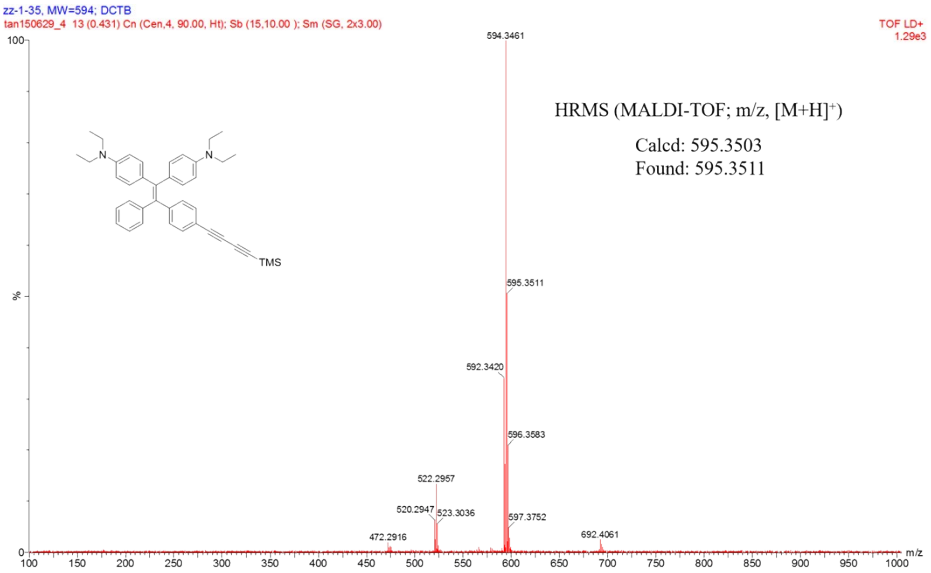

Figure S3. High resolution mass spectrum of compound **2**.

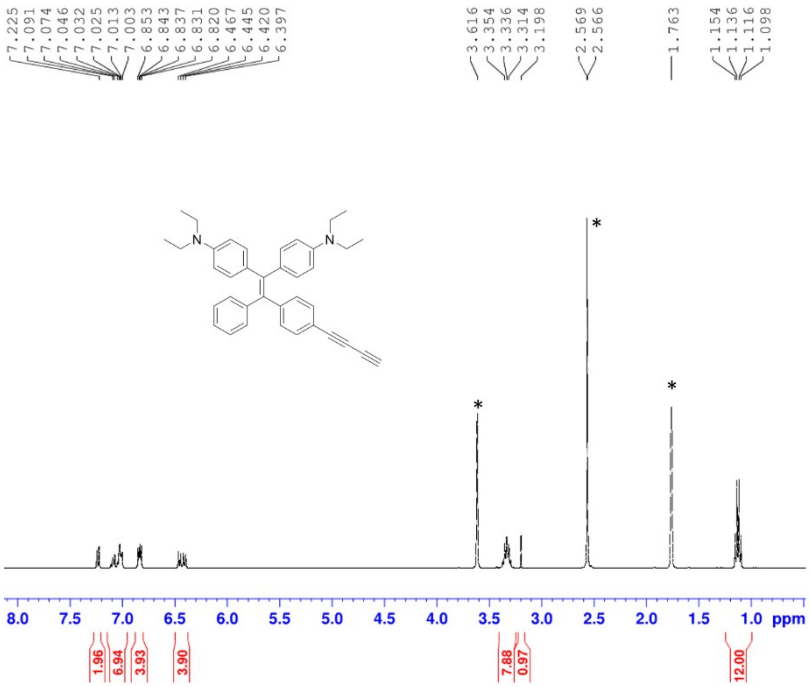

Figure S4. ^{1}H NMR spectrum of compound **1** inTHF-d_8.

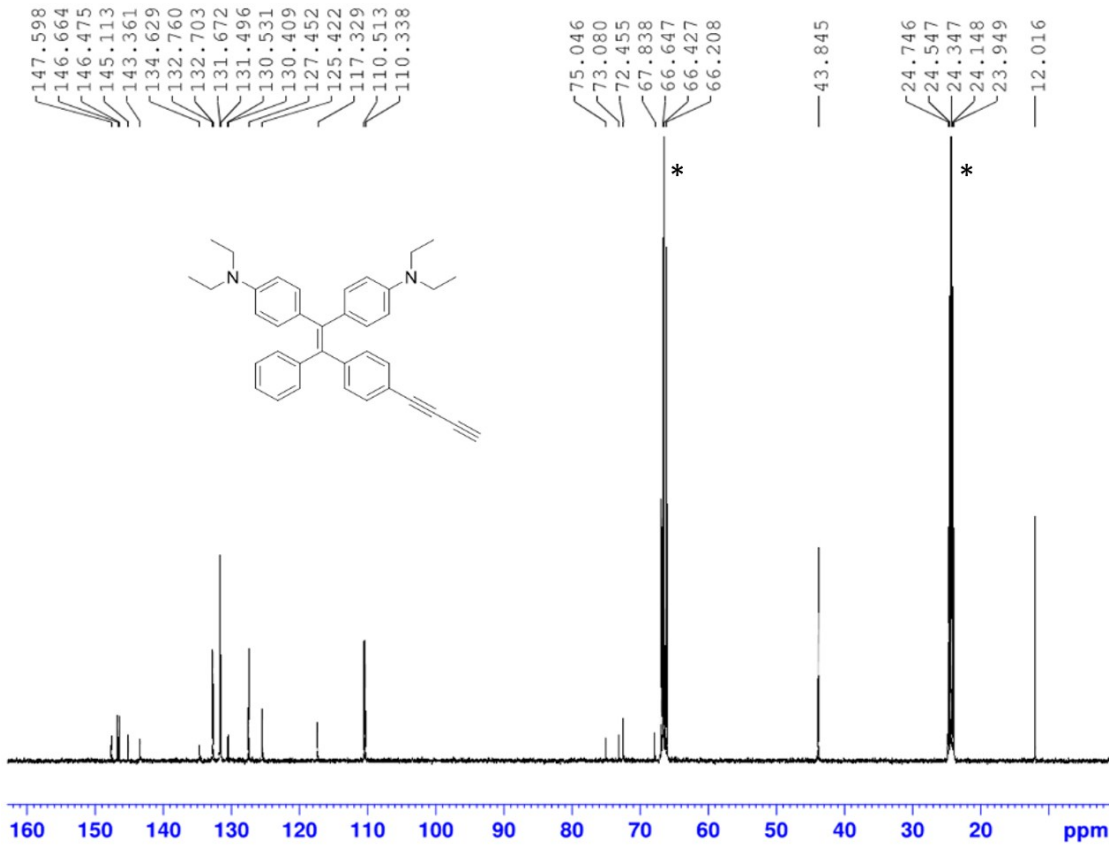

Figure S5. ^{13}C NMR spectrum of compound **1** inTHF-d_8.

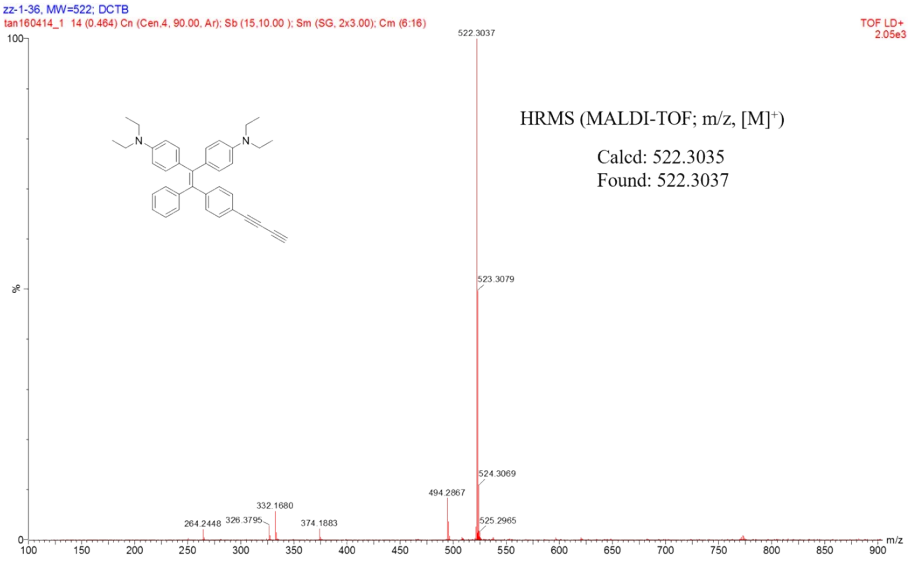

Figure S6. High resolution mass spectrum of compound **1**.

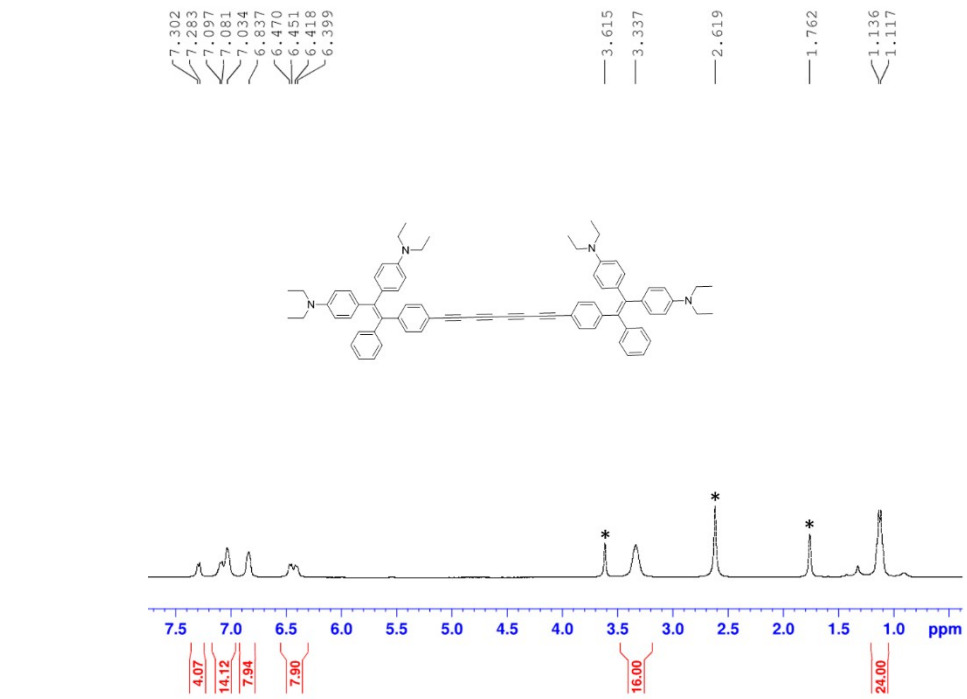

Figure S7. ^{1}H NMR spectrum of compound 2TPE-4E inTHF-d_8.

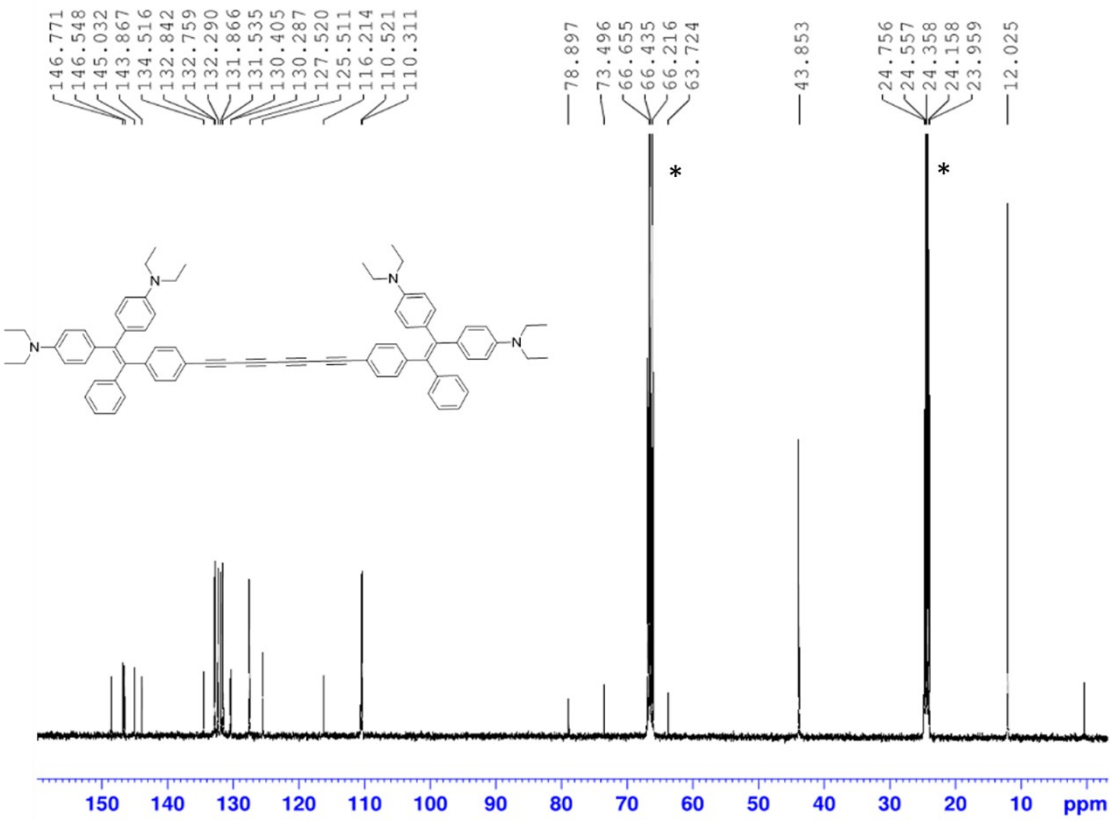

Figure S8. ^{13}C NMR spectrum of compound 2TPE-4E inTHF-d_8.

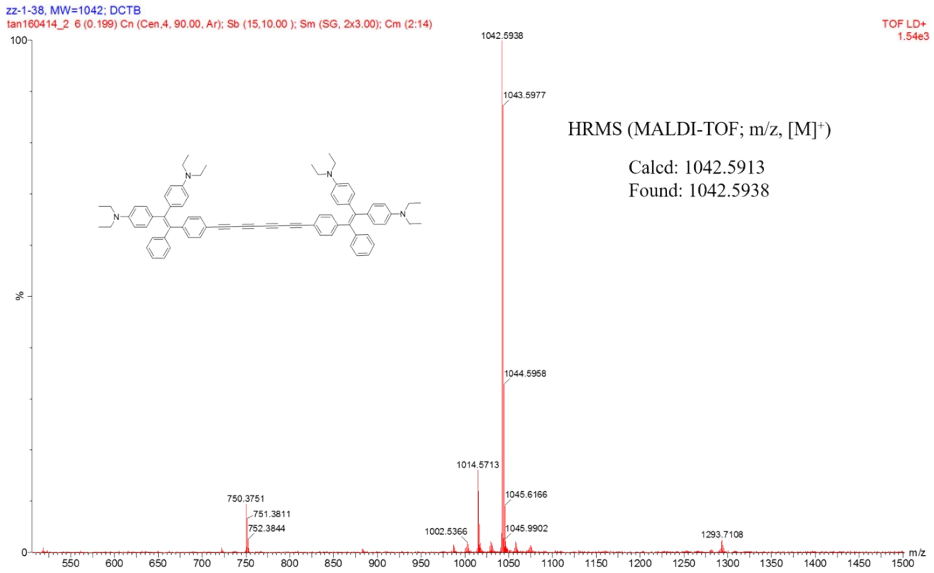

Figure S9. High resolution mass spectrum of compound 2TPE-4E.

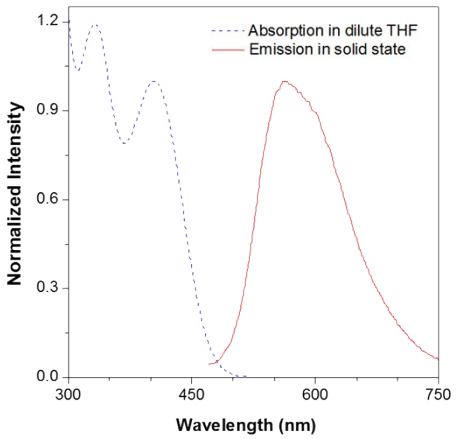

Figure S10. The absorption of compound **1** in dilute THF and its emission in solid state.

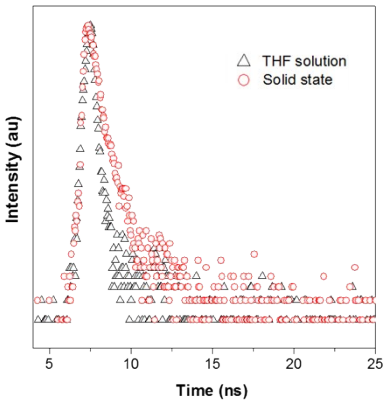

Figure S11. Fluorescence decay curves of 2TPE-4E in the solution and solid states.

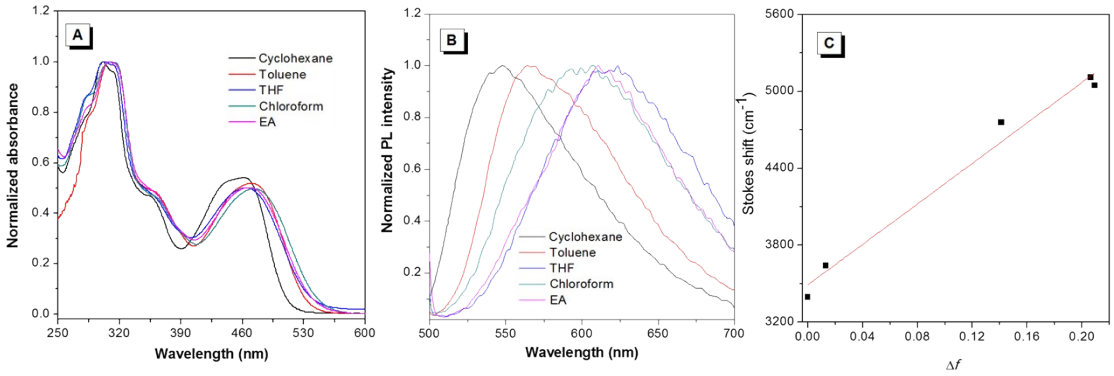

Figure S12. (A) Normalized UV/Vis and (B) PL spectra of 2TPE-4E spectra in solvents with different polarities. The absorption maximum of each solution was chosen as its excitation wavelength. (C) Plot of Stokes shift versus Δf of the solvent. Δf is defined as the change of dipole moment of the solute between the ground and excited states. Lippert–Mataga equation: $\nu_{abs} - \nu_{em} = 2(\Delta\mu^2/hca^3)\ \Delta f + \text{const.}$ ν_{abs} (ν_{em}) is the wavenumber of the absorption (fluorescence) maximum, h is the Planck constant, c is the light velocity, a is the radius of the Onsager cavity, and $\Delta f = (\varepsilon - 1)/(2\varepsilon + 1) - (n^2 - 1)/(2n^2 + 1)$, where ε is the dielectric constant and n the refractive index of the solvent.

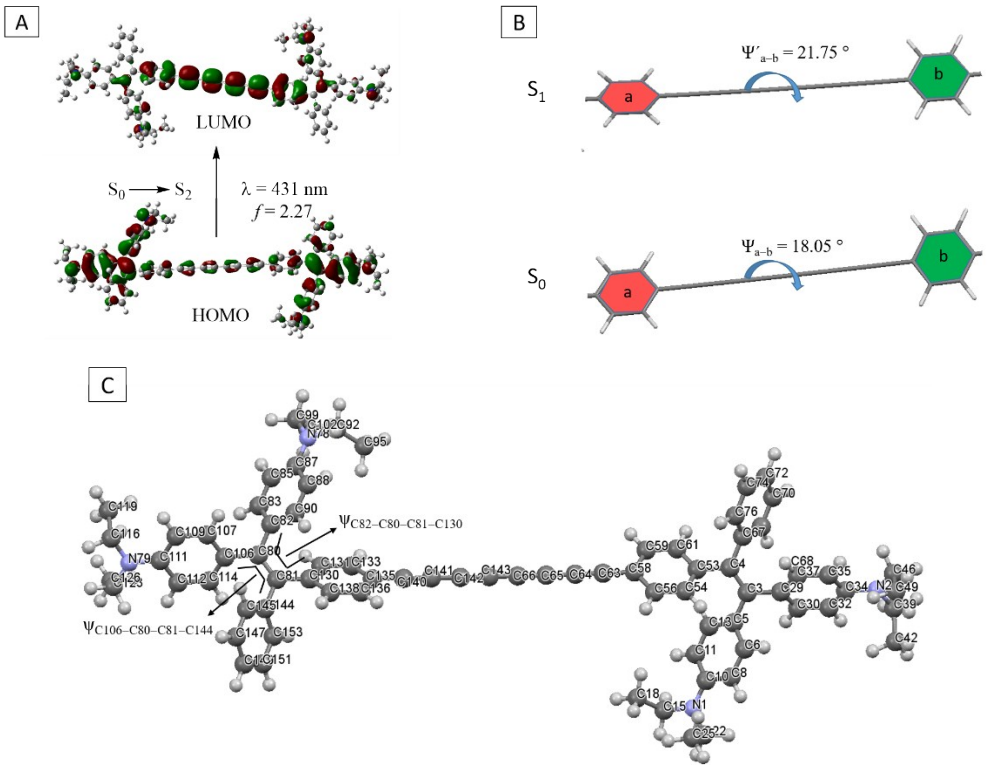

Figure S13. (A) Molecular orbitals, electronic transistions and oscillator strengths of 2TPE-4E by time dependent B3LYP/6-31G (d). (B) The twisted angle between the two pheny rings of the two sides of the polyyne moiety in the S_0 and S_1 state. (C) Optimized structure of 2TPE-4E with labels of carbon atoms.

Table S1. Selected Bond Lengths and Dihedral Angles in the Optimized Geometry of 2TPE-4E.

		S_0	S_1
Bond length (L)	C_{136}–C_{140}	1.425 Å	1.412 Å
	C_{140}–C_{141}	1.217 Å	1.248 Å
	C_{141}–C_{142}	1.365 Å	1.311 Å
	C_{142}–C_{143}	1.221 Å	1.289 Å
	C_{143}–C_{66}	1.362 Å	1.284 Å
Dihedral angle (θ)	C_{82}–C_{80}–C_{81}–C_{130}	12.41°	13.05°
	C_{106}–C_{80}–C_{81}–C_{144}	13.33°	13.34°

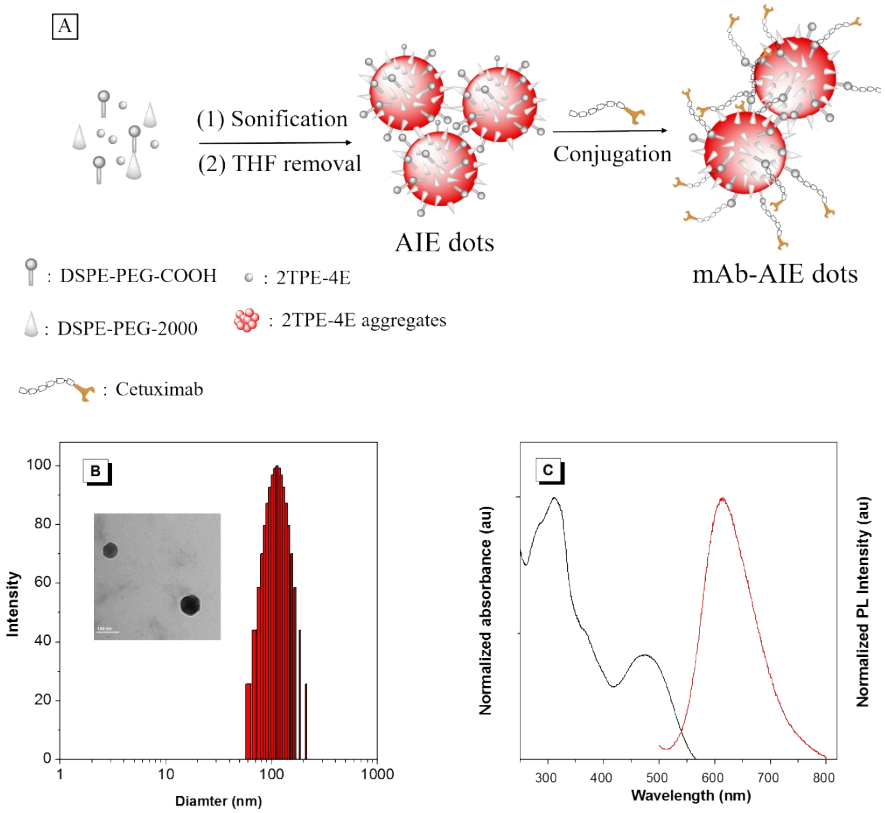

Figure S14. (A) Fabrication of mAb-AIE dots. (B) Particle size distribution and morphology of mAb-AIE dots studied by dynamic light scattering and high resolution transmission electron microscopy. (C) Absorption and emission spectra of mAb-AIE dots in water; λ_{ex} = 473 nm.

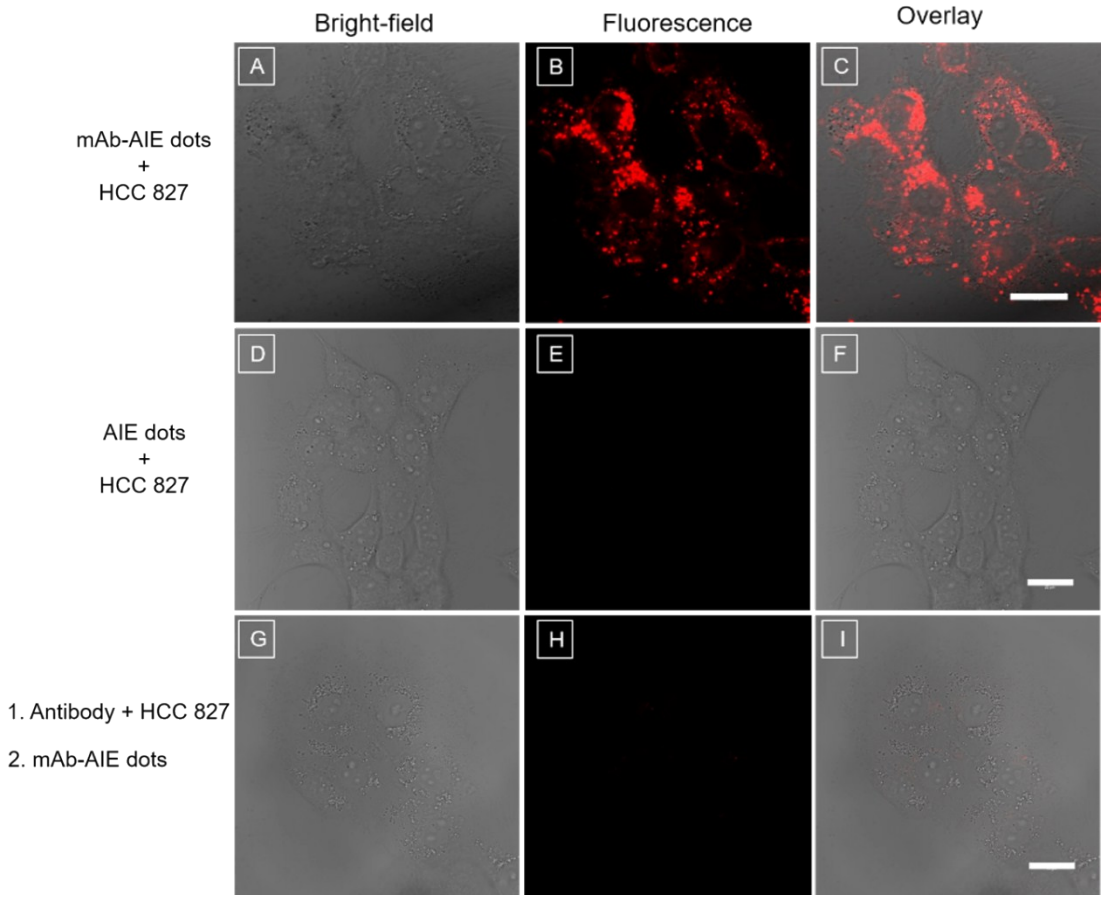

Figure S15 (A–I) Confocal images of HCC 827 cells with (A–C) mAb-AIE dots, (D–F) AIE dots and (G–I) first antibody followed by mAb-AIE dots for 6 h. Scale bar = 20 μm.

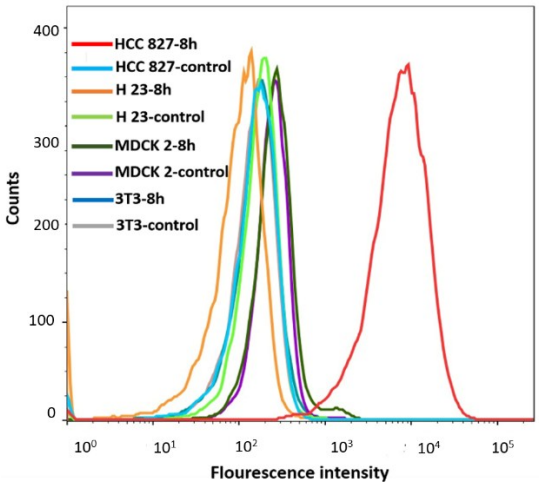

Figure S16. Flow cytometry histograms of HCC 827, NCI-H 23, NIH 3T3 and MDCK 2 cells incubated with mAb-AIE dots at 37 °C for 8 h.

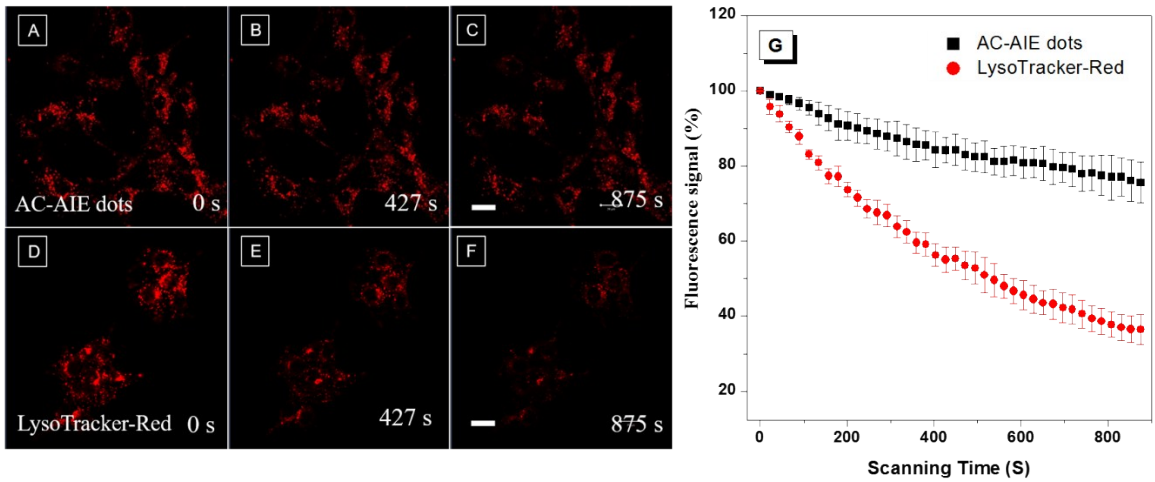

Figure S17. (A–F) Fluorescent images of HCC 827 cells incubated with (A–C) mAb-AIE dots and (D–F) LysoTracker-Red taken at different scanning times. (G) Fluorescence signal lost in dye-labled cells after continuous laser exposure for designated time intervals.

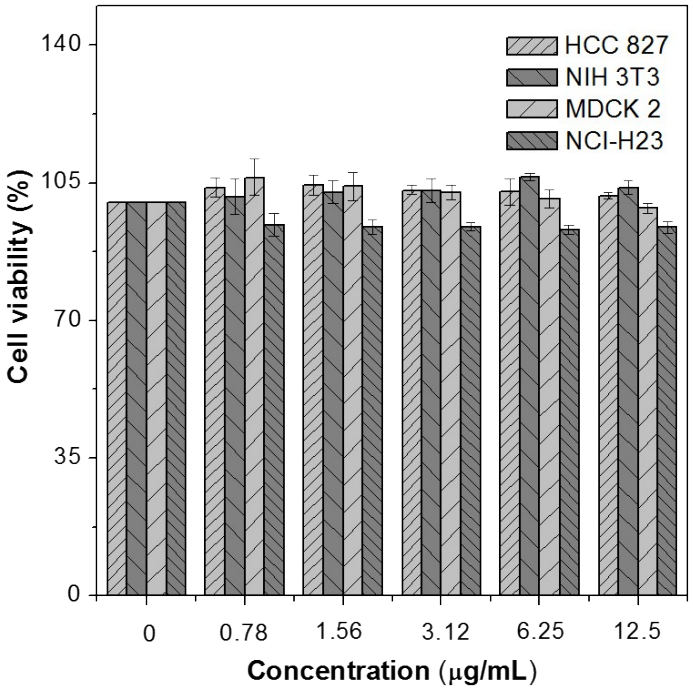

Figure S18. Cell viability of HCC 827, NIH 3T3, MDCK 2 and NCI-H23 cells treated with different concentrations of mAb-AIE dots.